Plasmonics - The Next Wave of Chip-scale Device Technologies

Rashid Zia, Jon Schuler, Anu Chandran, and Mark L. Brongersma
Geballe Laboratory for Advanced Materials,
Stanford University, Stanford, CA USA 94305

Abstract

The development of chip-scale electronics and photonics has led to remarkable data processing and transport capabilities that permeate almost every facet of our daily lives. Plasmonics is an exciting new device technology that has recently emerged. It exploits the unique optical properties of metallic nanostructures to enable routing and manipulation of light at the nanoscale. A tremendous synergy can be attained by integrating plasmonic, electronic, and conventional dielectric photonic devices on the same chip and taking advantage of the strengths of each technology.

The ever increasing demand for faster information transport and processing capabilities is undeniable. Our data hungry society has driven the enormous progress in the Si electronics industry and we have witnessed a continous progression towards smaller, faster, and more efficient electronic devices over the last five decades. Device scaling has also brought about a myriad of challenges. Currently, two of the most daunting problems preventing significant increases in processor speed are thermal and RC delay time issues associated with electronic interconnection [1-3]. Optical interconnects, on the other hand, possess an almost unimaginably large data carrying capacity and may offer interesting new solutions for circumventing these problems [4, 5]. Optical alternatives may be particularly attractive for future chips with more distributed architectures in which a multitude of fast electronic computing units (cores) need to be connected by high speed links. Unfortunately, their implementation is hampered by the large size mismatch between electronic and dielectric photonic components. Dielectric photonic devices are limited in size by the fundamental laws of diffraction to about half a wavelength of light and tend to be at least 1 or 2 orders of magnitude larger than their nanoscale electronic counterparts. This obvious size mismatch between electronic and photonic components presents a major challenge for interfacing these technologies. It thus appears that further progress will require the development of a radically new chip-scale device technology that can facilitate information transport between nanoscale devices at optical frequencies and bridge the gap between the world of *nanoscale* electronics and *microscale* photonics. In the following, we discuss a candidate technology that recently emerged [6, 7] and was termed "plasmonics" [8]. This device technology exploits the unique optical properties of nanoscale metallic structures to route and manipulate light at the nanoscale. A tremendous synergy could be attained by integrating plasmonic, electronic, and conventional photonic devices on the same chip and taking advantage of the strengths of each technology. In the following, we present some of our recent studies on plasmonic structures and conclude by providing an assessment of the potential opportunities and limitations for silicon chip-scale plasmonics.

Metal nanostructures may possess exactly the right combination of electronic and optical properties to tackle the issues outlined above and realize the dream of significantly faster processing speeds. The metals commonly used in electrical interconnection such as copper (Cu) and aluminum (Al) allow for the excitation of surface plasmon-polaritons (SPPs). SPPs are electromagnetic waves that propagate along a metal-dielectric interface and are coupled to the free electrons in the metal, as pictorially shown in Fig. 1 [9-11].
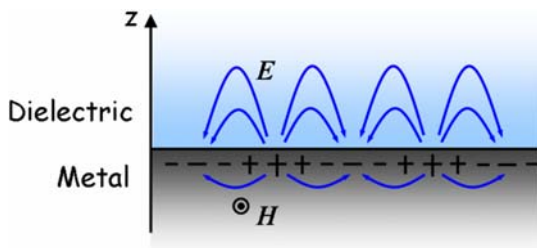

Figure 1. Surface plasmon-polariton (SPP) propagating along a metal-dielectric interface. These waves are transverse magnetic in nature. Their electromagnetic field intensity is highest at the surface and decays exponentially away from the interface. From an engineering standpoint a SPP can be viewed as a special type of light wave propagating along the metal surface.

From an engineering standpoint a SPP can be viewed as a special type of light wave and the metallic interconnects that support such waves thus serve as tiny optical waveguides, termed *plasmonic waveguides*. The notion that the optical mode ("light beam") diameter normal to the metal interface can be significantly smaller than the wavelength of light [12], has generated significant excitement and sparked the dream that *one day we will be able to interface nanoscale electronics with similar sized optical (plasmonic) devices.*

It is important to realize that with the latest advances in electromagnetic simulations and current CMOS compatible fabrication techniques a variety of functional plasmonic structures can be designed and fabricated in a Si foundry right now. Current silicon-based integrated circuit technology is already capable of making nanoscale metallic structures such as the copper and aluminum interconnects that route electronic signals between the transistors on a chip. This mature processing technology can thus also be used to our advantage to integrate plasmonic devices with their electronic and dielectric photonic counterparts. In some cases plasmonic waveguides may even perform a dual function and simultaneously carry both optical and electrical signals, giving rise to exciting new capabilities [13].

In order to study the propagation of SPPs, we constructed a photon scanning tunneling microscope (PSTM) [14] by modifying a commercially available scanning near-field optical microscope (α-SNOM; WITec GmbH; Ulm, Germany). PSTMs have been the tool of choice to characterize SPP propagation along extended films as well as metal stripe waveguides [15-17]. Figure 2(a) shows schematically how a microscope objective (Zeiss Alpha Plan-Fluar, 100X, NA=1.45) at the heart of our PSTM can be used to focus a laser beam onto a metal film at a well-defined angle and thereby launch a SPP along the top metal surface. This method of exciting SPPs makes use of the well-known Kretschmann geometry that enables phase matching of the free space excitation beam and the SPP [18].
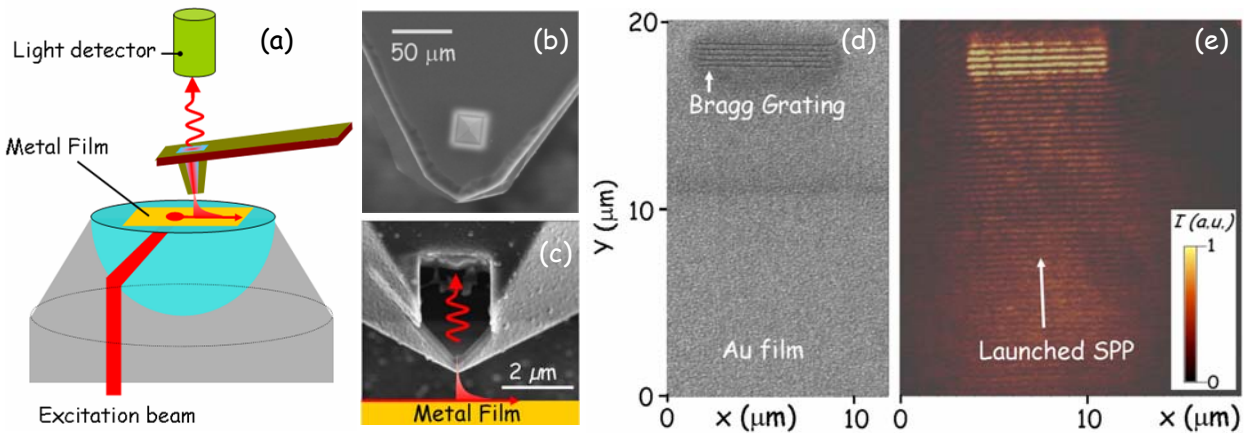

Figure 2. (a) Schematic of the operation of a photon scanning tunneling microscope (PSTM) that enables the study of surface plasmon-polariton (SPP) propagation along metal film surfaces. A red arrow shows pictorially how a SPP is launched from an excitation spot onto a metal film surface using a high numerical aperture microscope objective. (b) Scanning electron microscopy (SEM) image of the near-field optical cantilever probe used in our experiments. The tip consists of a micro-fabricated, hollow glass pyramid coated with an optically thick layer of aluminum. Light can be collected or emitted through a ~ 50 nm hole fabricated in the aluminum film on the top of the pyramid. (c) A cross-sectional view of the same hollow pyramidal tip, after a large section was cut out of the sidewall with a focused ion beam (FIB) tool. It is shown pictorially how the pyramidal tip in close proximity to the surface can tap into to propagating SPP and scatter out a little bit of light through the ~ 50 nm hole. The scattered light is detected in the far-field, providing a measure of the local field intensity right underneath the tip. By scanning the tip over the sample and measuring the intensity at each tip position, images of propagating SPP can be created. (d) Shows an SEM image of a Au film into which a Bragg grating was fabricated using a FIB. (e) A PSTM image of a SPP wave that was launched along the metal film toward the Bragg grating. The back reflection of the SPP from the Bragg grating results in the observed standing wave interference pattern.

A sharp, metal-coated, pyramidal tip, as shown in Fig. 2 (b) and (c), is used to locally *tap into* the guided SPP wave and scatter light towards a far-field detector. These particular tips have a nanoscale aperture defined on the top of the pyramid through which light can be collected. The scattered light is then detected with a photomultiplier tube. The detected signal provides a measure of the local light intensity right underneath the tip and by scanning the tip over the metal surface the propagation of SPPs can be imaged.

The operation of the PSTM can be illustrated nicely by investigating the propagation of SPPs on a patterned Au film, as shown in Figure 2 (d). Here, a focused ion beam (FIB) was used to define a series of parallel grooves serving as a Bragg grating that reflects SPP waves. Figure 2(e) shows the PSTM image of a SPP wave excited with a 785 nm wavelength laser and directed towards the Bragg grating. The back reflection of the SPP from the grating results in the observed standing wave interference pattern in the image. From this type of experiment the wavelength of SPPs can be determined in a straightforward manner and compared to theory. The PSTM can also be used to directly image SPP propagation in plasmonic structures and devices of more complex architecture to elucidate their behavior. This is quite different than typical characterization procedures for photonic devices in which a device is seen as a black box with input and output ports. In such cases, the device operation is inferred from responses measured at output ports resulting from different stimuli provided at input ports. The PSTM provides a clear advantage by providing a direct method to observe the inner workings of plasmonic devices, offering *a peek inside the box*.

The valuable information provided by PSTM measurements of plasmonic structures allows us to evaluate the usefulness of plasmonics for interconnection. Plasmonic stripe waveguides provide a natural starting point for this discussion as such stripes very closely resemble conventional metal interconnects. In this study, electron beam lithography was used to generate 55 nm thick Au stripes on a SiO_2 glass slide with stripe widths ranging from 5 μm to 50 nm. Au stripes are ideal for fundamental waveguide transport studies as they are easy to fabricate, do not oxidize, and exhibit a qualitatively similar plasmonic response to Cu and Al [19]. Figure 3 (a) shows an optical micrograph of a typical device consisting of a large Au area from which SPPs can be launched onto varying width metal stripes. An SEM of a 250 nm wide stripe is shown as an inset. The red arrow shows pictorially how light is launched from a focused laser spot into a 1 μm wide stripe.
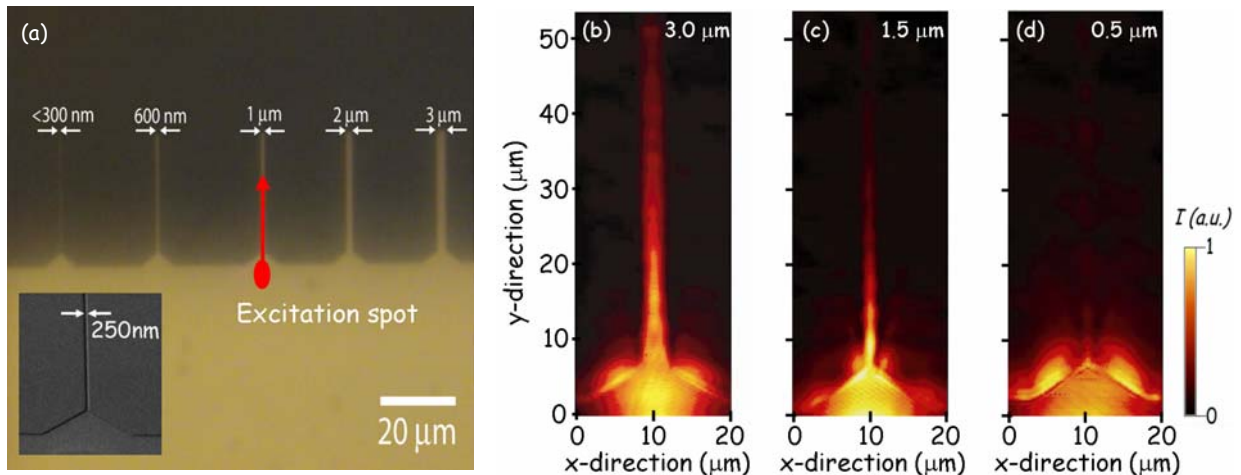

Figure 3. (a) Optical microscopy image of a SiO_2 substrate with an array of Au stripes attached to a large launchpad generated by electron beam lithography. The red arrow illustrates the launching of a surface plasmon-polariton (SPP) into a 1 μm wide stripe. (b), (c) , and (d) show PSTM images of SPPs excited at λ = 785 nm and propagating along 3.0 μm, 1.5μm, and 0.5 μm wide Au stripes, respectively.

Figure 3 (b), (c) , and (d) show PSTM images of SPPs excited at λ = 785 nm and propagating along 3.0 μm, 1.5 μm, and 0.5 μm wide Au stripes. The 3.0 μm wide stripe can be used to propagate signals over several tens of microns. Similar to previous far-field measurements along silver (Ag) stripes [20], it is clear that the propagation distance of SPPs decreases with decreasing stripe width. A better understanding of this behavior can be obtained from full-field simulations and a recently developed intuitive ray optics picture for plasmon waveguides [21-23].

Recent numerical work demonstrated that the modal solutions of plasmonic stripe waveguides are hybrid transverse electric-transverse magnetic (TE-TM) modes, and therefore, proper analysis requires numerical solution of the full vectorial wave equation [24-26]. To this end we developed a full vectorial magnetic field-finite difference method (FVH- FDM) for solving the electromagnetic Helmholtz equation [21, 27]. This is a frequency domain method and has clear advantages over the very popular finite difference time domain methods. One particularly attractive feature is that realistic, frequency dependent dielectric constants for the metals and dielectrics can be used as inputs to the simulation. Figure 4 shows two modal solutions obtained with this method for a 55 nm thick and 3.5 μm wide Au stripe on glass at λ=800 nm. It is worth noticing that SPP modes are supported on both the top and bottom Au surfaces. These waves can simultaneously carry information without interacting. The mode propagating along the top metal/air interface is called a leaky mode and the mode at the bottom metal/glass interface is called a bound mode. The field associated with these modes have a large H_x component, which is reminiscent of the purely TM nature of the SPP modes on infinite metal films. For this reason they are often called quasi-TM modes.
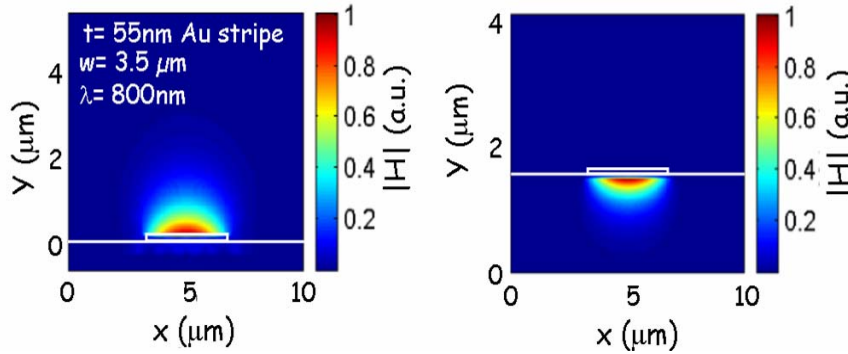

Figure 4. Simulated surface plasmon-pariton (SPP) mode profiles appropriate to a 55 nm thick and 3.5 μm wide Au stripe on a SiO₂ glass substrate. It shows both the leaky (left) and bound (right) SPP modes propagating at the top air/metal and bottom glass/ metal interfaces. Both modes can be employed simultaneously for information transport.

In addition to calculating the field intensity distributions of SPP modes, the FVH-FDM also provides values for the real and imaginary parts of the propagation constants. Figure 5 shows the complex propagation constants ($\beta_{sp} + i\ \alpha_{sp}$) determined for the lowest order leaky, quasi-TM modes supported by 55 nm thick Au stripes of various widths, W, at an excitation wavelength of 800 nm [21]. The inset in the bottom graph shows the geometry used in the simulations. For this simulation the dielectric properties of Au ($\varepsilon_{Au} = -26.1437 + 1.8497\ i$) at the excitation wavelength of λ = 800 nm were used [28].
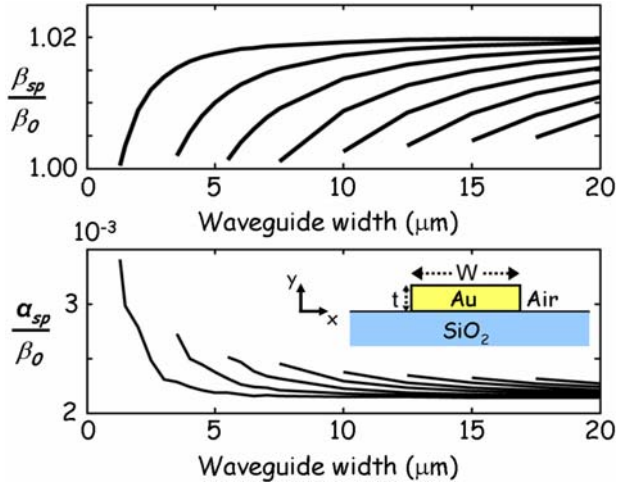
Figure 5. Calculated complex propagation constants ($\beta_{sp} + i\alpha_{sp}$) for the 8 lowest order leaky, quasi-TM surface plasmon-polariton modes of varying width Au stripe waveguides. For these calculations the Au stripe thickness was t = 55nm and the free space excitation wavelength was chosen to be λ = 800nm. The magnitudes of β_{sp} and α_{sp} were normalized to the real part of the free space propagation constant, β_0. The inset shows the simulated geometry and the coordinate frame.

Several important trends can be discerned from these plots. Similar to dielectric waveguides, larger structures tend to support an increased number of modes. Higher order SPP modes exhibit a higher number of maxima in the transverse magnetic field, H_x, along the x-direction. As the stripe width is decreased to a couple times the excitation wavelength, the wave number, β_{sp}, for all modes starts to decrease from the value of an infinitely wide stripe (β_{sp} = 1.02). The decrease of the propagation constant with decreasing stripe width first results in a reduced confinement of the modes and finally cutoff occurs for a width of ~1.3μm. At this width the SPP propagation constant has become equal to the propagation constant in air, β_0. The diminished confinement for narrow stripes results in a concomitant increase in the radiation losses into the high index SiO_2 substrate. This explains the larger α_{sp} observed for small stripe width. The 0.5 μm wide waveguide in Fig. 3 is below cutoff and does not support a quasi-TM mode. It appears, however, that there is a finite propagation length, which can be explained by taking into account the contribution to the measured field intensity from the radiation continuum (i.e. non-guided waves) [23]. It is important to note that simulations also predict cutoff for the bound modes, albeit at a slightly narrower stripe width [21].

The type of knowledge presented on the propagation behavior of plasmonic interconnects (mode size, propagation length, and cutoff) is essential for chip-designers and process engineers. It is clear that the short propagation distances found for plasmonic waveguides preclude direct competition with low-loss dielectric waveguide components. However, plasmonic structures can add new types of functionality to chips that cannot be obtained with dielectric photonics. One category of structures offering unique capabilities are active plasmonic interconnects. Such interconnects maybe offer new capabilities by introducing non-linear optical or electrical materials into otherwise passive plasmonic waveguides [29]. If the non-linearities are strong enough, these devices can be made small compared to characteristic decay lengths of SPPs and their performance parameters should not suffer from the unavoidable resistive losses in the metals.

While we have shown that weakly guided stripe waveguides cannot achieve deep sub-wavelength confinement, there exist alternative strongly guiding geometries which can provide markedly better confinement. For the discussion on novel interconnection schemes, this category of structures is of great interest. For example, Takahara's original paper on SPP modes of a metal cylinder show that subwavelength mode diameters are possible and propagation over short distances can be realized [12]. Waveguides consisting of two closely spaced metals also combine propagation distances of a few micron with deep sub-wavelength confinement [19, 30, 31]. Figure 6 (a) shows a comparison of the propagation lengths (1/e decay length in $|E_z|^2$) for planar metal\insulator\metal (MIM) waveguides and waveguides

5

consisting of a metal film sandwiched between two insulators (IMI waveguides). These calculations where performed using the well-established reflection pole method at the important telecom wavelength of 1.55 μm [32]. This technique, based on the transfer matrix formalism, monitors the phase of the reflection coefficient denominator, and can be used to solve for the complex propagation constants of both bound and leaky modes in lossy waveguides. We again used Au (ε_{Au} = -95.92 + i 10.97 at λ = 1.55 μm) as the metal and air as the insulator [28]. For a sufficiently large center layer thickness the propagation lengths for these two types of waveguides converge to the propagation length found for a single interface (dashed line in Fig. 6 (a)). This is reasonable since the SPP modes on the two metal surfaces decouple when the spacing between them becomes large. As the center layer thickness decreases and the SPPs at the two interfaces start to interact, the propagation length along MIM structures decreases while it increases along IMI structures. In fact, IMI waveguides can reach centimeter propagation distances for very thin metal films. For obvious reasons, these are termed long range SPP modes [33, 34]. These "large" propagation distances can be understood by realizing that the spatial extent of the modes at these extremely thin metallic film thicknesses becomes as large as 10 μm, as shown in Fig. 6(b). In that case the SPP waves are almost entirely propagating in the very low loss air region with very little field intensity inside the lossy (resistive) metal.
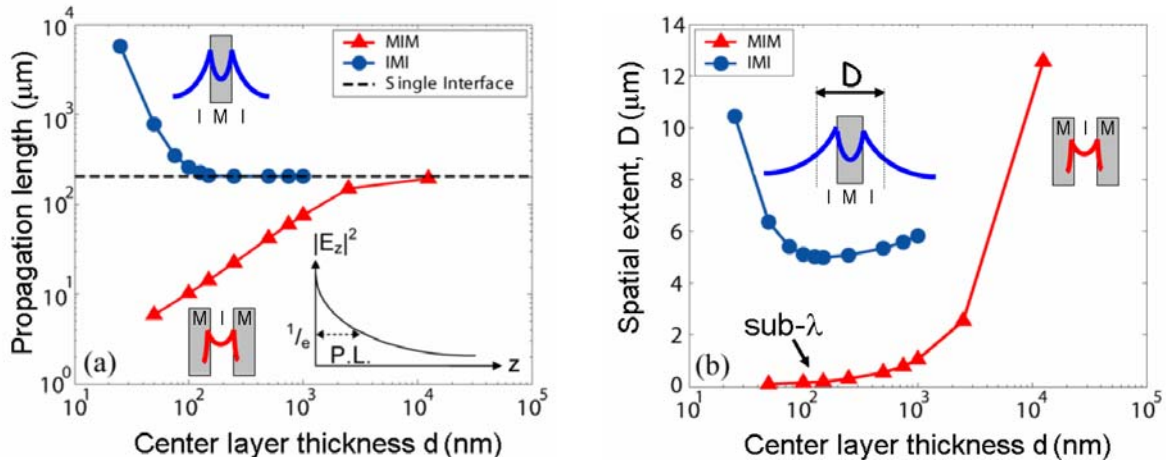

Figure 6. (a) Plot of the surface plasmon-polariton propagation length as a function of the center layer thickness for metal\insulator\metal MIM and insulator\metal\insulator (IMI) plasmonic waveguides. The calculations were performed of the (a) propagation length and (b) spatial extent of the SPP modes as a function of decreasing center layer thickness. The insets graphically illustrate plotted terms. The reflection pole method was used at λ = 1.55μm and Au was taken for the metal and air as the insulator

The MIM modes exhibit a continuous decrease in the propagation length as the center insulating layer thickness is reduced. However, Fig. 6 (b) shows that by "pushing" the metals closer together it is feasible to realize deep sub-wavelength mode diameters without running into problems with cutoff. For example, the spatial extent decreases to about 100nm ($< \lambda/15$) for metal to metal spacing of 50nm. It thus seems possible to transport information in a deep sub-wavelength mode over short (~ 1 μm) distances, which is impossible with conventional dielectric components. For CMOS compatible Cu and Al plasmonic waveguides similar numbers are found and were discussed in a recent publication [19]. Within the short propagation distances MIM structures also allow for routing of electromagnetic energy around sharp corners and split signals in T-junctions [35]. These unique features can be used to realize truly nanoscale photonic functionality and circuitry [36, 37], although the maximum size of such circuits will be limited in size by the SPP propagation length. It is important to realize that for every type of waveguide, there is

6

a clear, but different, trade-off between confinement and propagation distance (loss). The use of one type of waveguide over another will thus depend on application specific constraints.

Based on the data presented above, it seems that the propagation lengths for plasmonic waveguides are too short to propagate SPPs with high confinement over the length of an entire chip (~ 1cm). Although, the manufacturability of long-range SPP waveguides may well be straightforward within a CMOS foundry, it is unlikely that such waveguides will be able to compete with well-established, low-loss and high-confinement Si, Si_3N_4 or other dielectric waveguides [38-40]. However, it is possible to create new capabilities by capitalizing on an additional strongpoint of metallic nanostructures. Metal nanostructures have a unique ability to concentrate light into nanoscale volumes. This capability has been employed extensively to enhance a diversity of non-linear optical phenomena. For example, surface enhanced Raman scattering (SERS) is widely used in the field of biology [41-44]. This technique makes use of the enhanced electromagnetic fields near metallic nanostructures to study the structure and composition of organic and biological materials. Enhancement factors on the order of 100 have been predicted and observed for spherical particles. Even greater enhancements can be obtained near carefully engineered metal *optical antenna structures* that basically resemble scaled down versions of a car antenna [45]. Such antennas have recently even enabled single molecule studies by SERS and white-light supercontinuum generation [46-48].

Despite the numerous studies on antennas in the microwave and optical regimes, their application to solve current issues with chip-scale interconnection have remained largely unexplored. The field concentrating abilities of optical antennas may serve to bridge the large gap between microscale dielectric photonic devices and nanoscale electronics, as illustrated in Fig.7. This figure shows a detail of a chip on which optical signals routed through conventional dielectric optical waveguides. The mode size of such waveguides is typically at least one or two orders of magnitude larger than the underlying CMOS electronics. An antenna can be used to concentrate the electromagnetic signals from the waveguide mode into a deep subwavelength metal\insulator\metal waveguide and inject it into a nanoscale photodetector. The small size ensures a small capacitance, low-noise, high speed operation. By using metallic nanostructures as a bridge between photonics and electronics, one plays to the strengths of the metallic nanostructures (concentrating fields and subwavelength guiding), the dielectric waveguides (low loss information transport) and the nanoscale electronic components (high speed information processing).
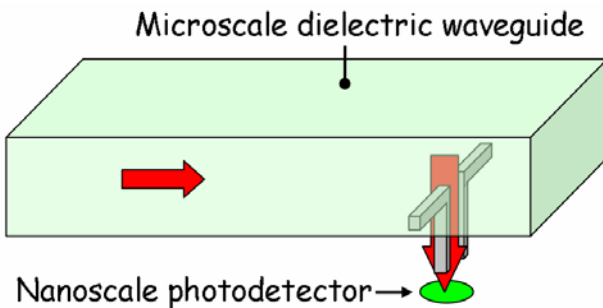

Figure 7. Schematic illustration how a nanoscale antenna structure can serve as a bridge between microscale dielectric components and nanoscale electronic devices.

Conclusions

Plasmonics has potential to play a unique and important role in enhancing the processing speed of future integrated circuitry. The field of plasmonics has witnessed an explosive growth over the last few years and our knowledge base in this area is rapidly expanding. As a result, the role of plasmonic devices on a chip is also becoming more well-defined and can be captured in the graph shown in Fig. 8. This graph shows the operating speeds and critical dimensions of different chip-scale device technologies. In

the past devices were relatively slow and bulky. The semiconductor industry has performed an incredible job at scaling electronic devices to nanoscale dimensions. Unfortunately, interconnect delay time issues may limit processing speeds of purely electronic integrated circuits. In stark contrast, photonic devices possess an enormous data carrying capacity (bandwidth). Unfortunately, dielectric photonic components are limited in their size by the fundamental laws of diffraction, preventing the same scaling that was possible for electronics. Finally, plasmonics offers precisely what electronics and photonics do not have: The size of electronics and the speed of photonics. Plasmonic devices might therefore naturally interface with similar speed photonic devices and with similar size electronic components. For these reasons, plasmonics may well serve as the *missing link* between two device technologies that have a difficult time communicating today. By increasing the synergy between these technologies, plasmonics may be able to unleash the full potential of nanoscale functionality and become the next wave of chip-scale technologies.
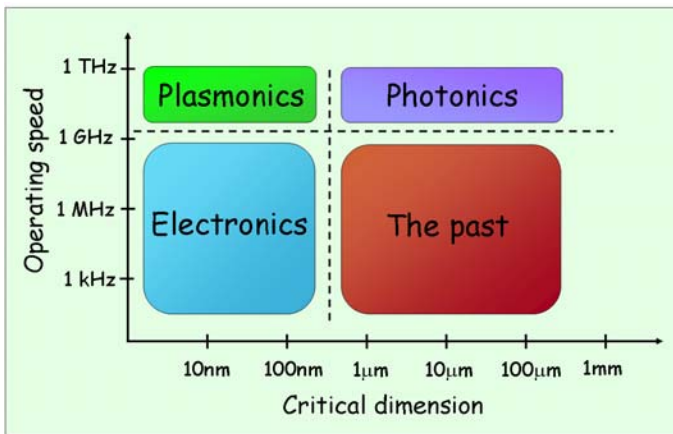
Figure 8. Graph of the operating speeds and critical dimensions of different chip-scale device technologies. This graph can be used to highlight the strengths of different chip-scale device technologies.

Acknowledgements

References

1. Bohr, M.T., *Interconnect Scaling – The Real Limiter to High Performance ULSI.* Tech. Dig. IEDM, 1995: p. 241-244
2. Chiang, T.-Y., B. Shieh, and K.C. Saraswat, *Impact of joule heating on scaling of deep sub-micron Cu/low-k interconnects.* IEEE Symposium on VLSI Circuits, Digest of Technical Papers, 2002: p. 38-39.
3. K. Banerjee, A.A., G. Dixit, and C. Hu, *The Effect of Interconnect Scaling and Low-k Dielectric on the Thermals Characteristics of the IC Metal* Tech. Dig. IEDM, 1996: p. 65-68
4. Miller, D.A.B., *Rationale and challenges for optical interconnects to electronic chips.* Proceedings of the IEEE, 2000. **88**(6): p. 728-49.
5. Chen, G., et al., *Predictions of CMOS compatible on-chip optical interconnect.* International Workshop on System Level Interconnect Prediction, SLIP, 2005: p. 13-20.
6. Barnes, W.L., A. Dereux, and T.W. Ebbesen, *Surface plasmon subwavelength optics.* Nature, 2003. **424**(6950): p. 824-830.
7. Takahara, J. and T. Kobayashi, *Low-dimensional optical waves and nano-optical circuits.* Optics & Photonics News, 2004. **15**(10): p. 54-9.

8.   Brongersma, M.L., J.W. Hartman, and H.H. Atwater. *Plasmonics: electromagnetic energy transfer and switching in nanoparticle chain-arrays below the diffraction limit*. in *Molecular Electronics. Symposium, 29 Nov.-2 Dec. 1999, Boston, MA, USA*. 1999: Warrendale, PA, USA : Mater. Res. Soc, 2001, This reference contains the first occurrence of the word "Plasmonics" in the title, subject, or abstract in the Inspec ® database.

9.   Economou, E.N., *Surface plasmons in thin films*. Physical Review, 1969. **182**(2): p. 539-54.

10. Raether, H., *Surface plasmons on smooth and rough surfaces and on gratings*. 1988, New York: Springer-Verlag.

11. Burke, J.J., G.I. Stegeman, and T. Tamir, *Surface-polariton-like waves guided by thin, lossy metal films*. Physical Review B (Condensed Matter), 1986. **33**(8): p. 5186-201.

12. Takahara, J., et al., *Guiding of a one-dimensional optical beam with nanometer diameter*. Optics Letters, 1997. **22**(7): p. 475-7.

13. Nikolajsen, T., K. Leosson, and S.I. Bozhevolnyi, *In-line extinction modulator based on long-range surface plasmon polaritons*. Optics Communications, 2005. **244**(1/6): p. 455-9.

14. Reddick, R.C., R.J. Warmack, and T.L. Ferrell, *New form of scanning optical microscopy*. Physical Review B (Condensed Matter), 1989. **39**(1): p. 767-70.

15. Weeber, J.C., et al., *Near-field observation of surface plasmon polariton propagation on thin metal stripes*. Physical Review B (Condensed Matter and Materials Physics), 2001. **64**(4): p. 045411-9.

16. Weeber, J.C., Y. Lacroute, and A. Dereux, *Optical near-field distributions of surface plasmon waveguide modes*. Physical Review B (Condensed Matter and Materials Physics), 2003. **68**(11): p. 115401-1.

17. Krenn, J.R., et al., *Non-diffraction-limited light transport by gold nanowires*. Europhysics Letters, 2002. **60**(5): p. 663-9.

18. Kretschmann, E., *The determination of the optical constants of metals by excitation of surface plasmons*. Zeitschrift fur Physik A (Atoms and Nuclei), 1971. **241**(4): p. 313-24.

19. Zia, R., et al., *Geometries and materials for subwavelength surface plasmon modes*. Journal of the Optical Society of America A: Optics and Image Science, and Vision, 2004. **21**(12): p. 2442-2446.

20. Lamprecht, B., et al., *Surface plasmon propagation in microscale metal stripes*. Applied Physics Letters, 2001. **79**(1): p. 51-3.

21. Zia, R., M.D. Selker, and M.L. Brongersma, *Leaky and bound modes of surface plasmon waveguides*. Physical Review B (Condensed Matter and Materials Physics), 2005. **71**(16): p. 165431-1.

22. Zia, R., A. Chandran, and M.L. Brongersma, *Dielectric waveguide model for guided surface polaritons*. Optics Letters, 2005. **30**(12): p. 1473-1475.

23. Zia, R., J.A. Schuller, and M.L. Brongersma, *Near-field characterization of guided polariton propagation and cutoff in surface plasmon waveguides*. Physical Review B, submitted 2006.

24. Al-Bader, S.J., *Optical transmission on metallic wires-fundamental modes*. IEEE Journal of Quantum Electronics, 2004. **40**(3): p. 325-9.

25. Berini, P., *Plasmon-polariton waves guided by thin lossy metal films of finite width: Bound modes of symmetric structures*. Physical Review B, 2000. **61**(15): p. 10484-10503.

26. Berini, P., *Plasmon-polariton waves guided by thin lossy metal films of finite width: Bound modes of asymmetric structures*. Physical Review B (Condensed Matter and Materials Physics), 2001. **63**(12): p. 125417-15.

27. Lusse, P., et al., *Analysis of vectorial mode fields in optical wave-guides by a new finite-difference method*. Journal of Lightwave Technology, 1994. **12**(3): p. 487-494.

28. Palik, E.D., *Handbook of Optical Constants of Solids*. 1985: Orlando, FL, USA : Academic Press, 1985. xviii, 804p.

29. Krasavin, A.V. and N.I. Zheludev, *Active plasmonics: controlling signals in Au/Ga waveguide using nanoscale structural transformations*. Applied Physics Letters, 2004. **84**(8): p. 1416-18.

30. Bozhevolnyi, S.I., et al., *Channel plasmon-polariton guiding by subwavelength metal grooves*. Physical Review Letters, 2005. **95**(4): p. 046802-4.

31. Veronis, G. and S.H. Fan, *Guided subwavelength plasmonic mode supported by a slot in a thin metal film*. Optics Letters, 2005. **30**(24): p. 3359-61.

32. Anemogiannis, E., E.N. Glytsis, and T.K. Gaylord, *Determination of guided and leaky modes in lossless and lossy planar multilayer optical waveguides: reflection pole method and wavevector density method*. Journal of Lightwave Technology, 1999. **17**(5): p. 929-41.

33. Sarid, D., *Long-range surface-plasma waves on very thin metal films.* Physical Review Letters, 1981. **47**(26): p. 1927-30.
34. Yang, F.Z., G.W. Bradberry, and J.R. Sambles, *Long-range surface mode supported by very thin silver films.* Physical Review Letters, 1991. **66**(15): p. 2030-2.
35. Veronis, G. and S.H. Fan, *Bends and splitters in metal-dielectric-metal subwavelength plasmonic waveguides.* Applied Physics Letters, 2005. **87**(13): p. 131102-1.
36. Tanaka, K. and M. Tanaka, *Simulations of nanometric optical circuits based on surface plasmon polariton gap waveguide.* Applied Physics Letters, 2003. **82**(8): p. 1158-60.
37. Bozhevolnyi, S.I., et al., *Channel plasmon subwavelength waveguide components including interferometers and ring resonators.* Nature, 2006. **440**(7083): p. 508-511.
38. Lee, K.K., et al., *Fabrication of ultralow-loss Si/SiO{sub 2} waveguides by roughness reduction.* Optics Letters, 2001. **26**(23): p. 1888-90.
39. Daldosso, N., et al., *Comparison among various Si{sub 3}N{sub 4} waveguide geometries grown within a CMOS fabrication pilot line.* Journal of Lightwave Technology, 2004. **22**(7): p. 1734-40.
40. Sparacin, D.K., S.J. Spector, and L.C. Kimerling, *Silicon waveguide sidewall smoothing by wet chemical oxidation.* Journal of Lightwave Technology, 2005. **23**(8): p. 2455-61.
41. Felidj, N., et al., *Optimized surface-enhanced Raman scattering on gold nanoparticle arrays.* Applied Physics Letters, 2003. **82**(18): p. 3095-7.
42. Shafer-Peltier, K.E., et al., *Toward a glucose biosensor based on surface-enhanced Raman scattering.* Journal of the American Chemical Society, 2003. **125**(2): p. 588-593.
43. Haynes, C.L. and R.P. Van Duyne, *Plasmon-sampled surface-enhanced Raman excitation spectroscopy.* Journal of Physical Chemistry B, 2003. **107**(30): p. 7426-7433.
44. Drachev, V.P., et al., *Surface-enhanced raman difference between human insulin and insulin lispro detected with adaptive nanostructures.* Journal of Physical Chemistry B, 2004. **108**(46): p. 18046-18052.
45. Crozier, K.B., et al., *Optical antennas: resonators for local field enhancement.* Journal of Applied Physics, 2003. **94**(7): p. 4632-42.
46. Nie, S.M. and S.R. Emery, *Probing single molecules and single nanoparticles by surface-enhanced Raman scattering.* Science, 1997. **275**(5303): p. 1102-6.
47. Kneipp, K., et al., *Single molecule detection using surface-enhanced Raman scattering (SERS).* Physical Review Letters, 1997. **78**(9): p. 1667-70.
48. Fromm, D.P., et al., *Exploring the chemical enhancement for surface-enhanced Raman scattering with Au bowtie nanoantennas.* Journal of Chemical Physics, 2006. **124**(6).